IEEE Access
Multidisciplinary | Rapid Review | Open Access Journal

Received June 20, 2019, accepted July 7, 2019, date of publication July 18, 2019, date of current version August 1, 2019.

Digital Object Identifier 10.1109/ACCESS.2019.2929746

A Widely Tunable Compact Bandpass Filter Based on a Switched Varactor-Tuned Resonator

MINJAE JUNG, (Student Member, IEEE), AND BYUNG-WOOK MIN, (Member, IEEE)
School of Electrical and Electronic Engineering, Yonsei University, Seoul 03722, South Korea

Corresponding author: Byung-Wook Min (bmin@yonsei.ac.kr)

This work was supported in part by the Basic Science Research Program and Space Core Technology Program through the National Research Foundation of Korea (NRF), Ministry of Science and ICT, under Grant 2017R1A1A1A05001134 and Grant 2017M1A3A3A02016255.

ABSTRACT This paper presents a compact tunable bandpass filter (BPF) based on a switched varactor tuned resonator with a wide frequency-tuning range and a constant absolute bandwidth (ABW). The proposed switched varactors are adopted to overcome the limited tunability of varactor diodes by switching the stubs. The pass-band can be easily tuned by controlling two resonant frequencies of each state. After the separation of the two resonant frequencies, the ABW of the filter is maintained constant by tuning the external coupling of the tapped-line input and output matching capacitors. To verify the proposed structure, a two-pole tunable BPF has been fabricated and measured. It exhibits a low in-band insertion loss of 1.4−2.9 dB, maintaining a constant 3-dB ABW of 75 MHz with a large tuning range from 255 to 725 MHz (1:2.85). The proposed two-pole filter shares the resonator for the low- and high-band states, and therefore the overall size is only $0.2\lambda_g \times 0.14\lambda_g$. In addition, this two-pole tunable filter is extended to a four-pole tunable one as an estimation of the measured results by using the simulated results. They have the wide frequency tuning ratios of 2.85 and 2.92, with the low insertion losses, respectively.

INDEX TERMS Constant absolute bandwidth, switched varactor, tunable resonator, tunable filter, wide tuning range.

I. INTRODUCTION

IN recent wireless communication systems, tunable filters with a wide frequency tuning range are increasingly required. The filters in mobile phones range from 700 MHz to 2.7 GHz, and need to be combined and tunable for software-defined radio systems [1]. Spectrum sensing, which is important for sharing and accessing spectrum dynamically, requires tunable filters to relax the linearity requirement of sensing receivers [2]. Because of the wide frequency range to be sensed and accessed, the frequency-tuning range of tunable filters needs to be as wide as possible. The bandwidth of tunable bandpass filters (BPFs) can change with the tuned center frequency, and the absolute bandwidth (ABW) or fractional bandwidth can be fixed by varying the coupling coefficient [3]. Considering the fixed (absolute) bandwidth of communication standards and systems, tunable filters with a constant ABW are the focus of many studies [4]–[6].

Many types of planar tunable filters have been developed in [7]–[14]. The tuning elements are generally solid-state varactors, and the frequency tuning ranges of filters are limited in practical because of the tuning range of the used varactors unless the filter is designed using microelectromechanical system (MEMS) devices [15], [16]. To increase the tuning range, several configurations have been proposed such as a switchable filter bank, zero-value coupling and switchable resonator. For the switchable filter banks, tunable filters with different frequency ranges and two channel switches are needed, which causes a large footprint from the filters that are not always in use, and a loss from the switches [17]. The switches, and therefore their loss, can be eliminated by zero-value coupling [18], [19], but there are still multiple filters/resonators to cover low and high bands, resulting in a large overall filter size. To reduce the overall size, specific parts of a resonator can be eliminated using RF switches, such as p-i-n diodes or transistor switches [5]. However, the design method is very complicated when it comes to obtaining a desired ABW with a wide tuning range. To circumvent the above shortcomings, tuning elements with a high tuning range need to be employed in the tunable filter.

In this paper, we present a tunable filter that has a wide frequency tuning ratio exceeding one octave (2.85). It is

The associate editor coordinating the review of this manuscript and approving it for publication was Qingfeng Zhang.

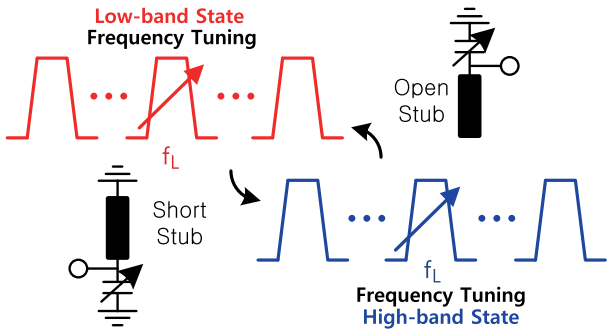

FIGURE 1. Concept of the proposed tunable BPF.

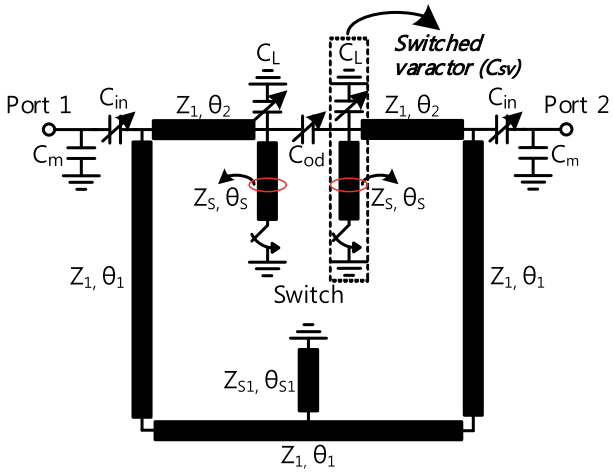

FIGURE 2. Configuration of the proposed tunable BPF.

compact owing to the use of proposed switched varactors, and can cover a wide frequency range continuously. As shown in Fig 1, the filter was designed to be switched between low-band (open stub-loaded varactor), and high-band (short stub-loaded varactor) states with a single resonator, resulting in a compact size. The filter is also tunable with varactor diodes in both states. To keep the ABW constant, two resonant frequencies are set for them to have the same separation. Coupling of the tapped-line input and output networks were carefully controlled. The proposed filter was fabricated and measured for demonstration, and exhibits a tuning range from 255 MHz to 725 MHz with a very low insertion loss of less than 2.9 dB showing a good agreement with the simulated results.

II. DESIGN THEORY AND ANALYSIS

Fig. 2 presents the configuration of the proposed tunable BPF designed by using switched varactors. To achieve a wide frequency tuning range, we firstly propose and utilize the concept of the switched varactor. The equivalent circuit of the proposed filter is shown in Fig. 3 where the parallel connection of C_L and switch-loaded stub (Z_s, θ_s) is transformed into the switched varactor (C_{sv}). When the switches are off (off state), the switched varactors are designated as $C_{sv.off}$, while these varactors are expressed as $C_{sv.on}$ when the switches are on (on state). In this section, the theoretical

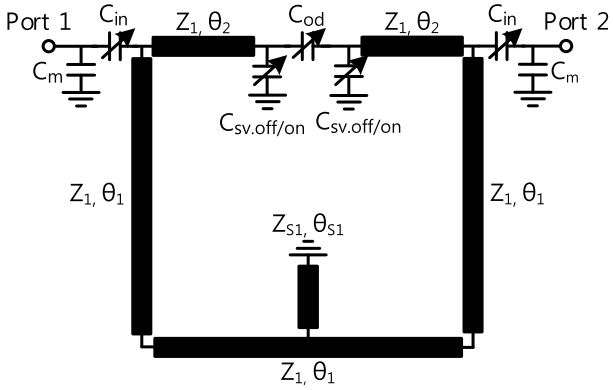

FIGURE 3. Equivalent circuit of the proposed filter.

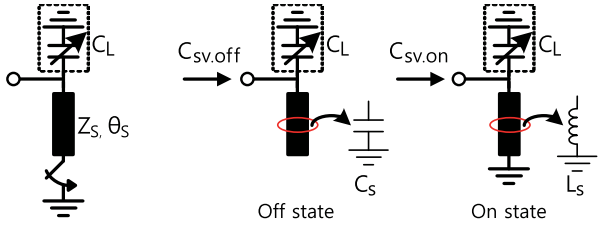

FIGURE 4. Concept of the proposed switched varactor.

analysis of the switched varactor and its application to a tunable resonator are presented. Then, the required external coupling is described to implement a tunable BPF with a constant ABW. Lastly, we summarize the design procedure of the proposed tunable BPF.

A. ANALYSIS OF THE SWITCHED VARACTOR

Fig. 4 shows the concept of the proposed switched varactor included in the tunable BPF to overcome the limited tunability of varactor diodes. By switching on and off the ground connection of the stub (Z_s), the short and open stubs can be modeled as an equivalent inductor (L_s=$Z_s$tanθ_s/ω) and a capacitor (C_s=tan$\theta_s/Z_s\omega$), respectively. The total capacitance (C_{sv}) of the switched varactor can be varied by the varactor C_L and switched between $C_{sv.on}$ and $C_{sv.off}$, which can be expressed as:

$$C_{L1} - \frac{1}{\omega^2 L_s} \le C_{sv.on} \le C_{L2} - \frac{1}{\omega^2 L_s} \quad (1a)$$

$$C_{L1} + C_s \le C_{sv.off} \le C_{L2} + C_s \quad (1b)$$

where C_{L1} and C_{L2} are the minimum and maximum capacitances of C_L, respectively. To have a continuous tuning range of the switched varactor and filter, the maximum value of $C_{sv.on}$ needs to be equal or larger than the minimum value of $C_{sv.off}$ at a transit frequency (f_t). The tunable filter can be tuned to f_t by both $C_{sv.on}$ and $C_{sv.off}$. Thus, the tuning range of C_{sv} is from $[C_{L1} - 1/(\omega_{max}^2 L_s)]$ to $[C_{L2} + C_s]$ where w_{max} is the highest angular tuned center frequency of the tunable filter, and $C_{L1} > 1/(\omega_{max}^2 L_s)$. To illustrate the operation of the switched varactor visually, the effective capacitance tuning curves of $C_{sv.off}$ and $C_{sv.on}$ are depicted on the left and

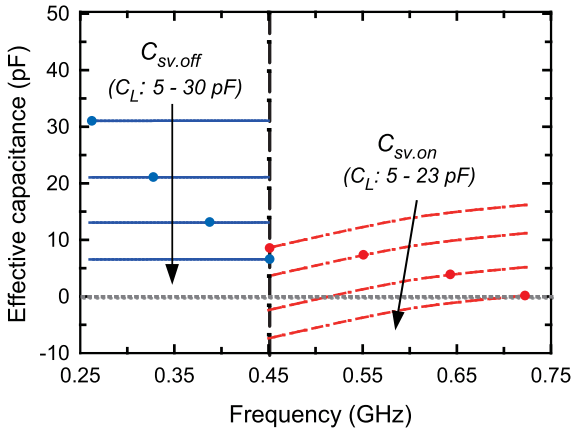

FIGURE 5. Capacitance tuning curve of the switched varactor.

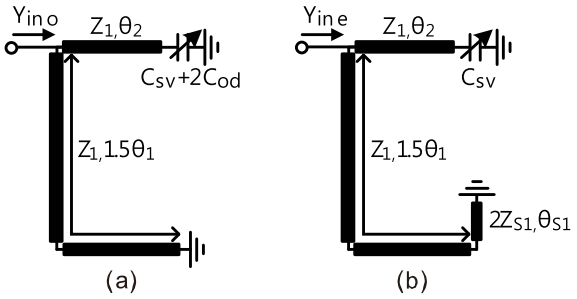

FIGURE 6. Equivalent circuits for the proposed dual-mode resonator. (a) odd-mode and (b) even-mode.

right side from the boundary designated at f_t, respectively as shown in Fig. 5. As explained earlier, it can be seen that the maximum value of $C_{sv.on}$ is larger than the minimum value of $C_{sv.off}$ at f_t of 450 MHz for a continuously wide tuning. In this design, C_L can vary from 5 pF to 30 pF when switch is off, and vary from 5 pF to 23 pF when switch is on with Z_s=95 Ω, and θ_s=15.4° at f_t of 450 MHz chosen to obtain C_s=1.03 pF and L_s=9.25 nH. As a result, C_{sv} is 6 pF at f_t=450 MHz varying from 0.1 pF at 730 MH to 31 pF at 250 MHz. This leads to an effective capacitance tuning ratio of 1:310 over the frequency tuning range. It can be expected that the tuning ratio of the filter is also improved significantly by using the proposed switched varactor. The application of the proposed varactor to the design of tunable resonator is demonstrated in the following subsection.

B. RESONANCE PROPERTIES OF THE PROPOSED RESONATOR

Because the proposed switched varactor tuned resonator is symmetrical in structure, even- and odd-mode analysis can be performed to explain the operation of each resonant frequency. Using the equivalent circuit models depicted in Fig. 6, the input admittances of the odd-mode and even-mode equivalent circuits can be written as

$$Y_{ino} = jY_1\{\frac{2Y_1\tan\theta_2 + j\omega(C_{sv}+2C_{od})}{2Y_1 - j\omega(C_{sv}+2C_{od})\tan\theta_2} - \cot(1.5\theta_1)\} \quad (2a)$$

TABLE 1. Electrical parameters of the proposed resonator.

Z_1	θ_1	θ_2	Z_{s1}	θ_{s1}	Z_s	θ_s
35 Ω	17.6°	7.1°	65 Ω	5.9°	95 Ω	15.4°

All electrical lengths are defined at 450 MHz.

$$Y_{ine} = jY_1\{\frac{2Y_1\tan\theta_2 + j(\omega C_{sv})}{2Y_1 - j(\omega C_{sv})\tan\theta_2} + \frac{2Y_1\tan(1.5\theta_1) + Y_S}{2Y_1 - Y_S\tan(1.5\theta_1)}\} \quad (2b)$$

$$Y_S = -j(0.5Y_{S1})\cot\theta_{S1} \quad (2c)$$

where C_{sv} varies in the range of (1). The odd- and even-mode resonant frequencies can be found when $Y_{ino}=0$, and $Y_{ine}=0$, respectively. Adjusting Z_{S1} and θ_{S1} can determine the location of the initial even-mode resonant frequency. From (2), it is obvious that the odd-mode resonant frequency can be affected by varying C_{sv} and C_{od}, while the even-mode resonant frequency can be relocated only by C_{sv}. Therefore, the resonant frequencies of the switched varactor tuned resonator can be tuned by C_{sv} and C_{od} can be used to control the separation between the odd- and even-mode resonant frequencies for a constant ABW.

To investigate the above analysis of the proposed resonator, its resonant feature is depicted graphically in Fig. 7, and is obtained by weak coupling excitation where the nominal electrical parameters at 450 MHz are selected, as listed in Table 1. Resonant frequencies, $f_{odh,LB/HB}$ and $f_{evh,LB/HB}$ in Fig. 7 denote the highest odd-mode and even-mode resonant frequencies in the low/high-band states, respectively. As described before, Z_S and θ_S can determine the effective capacitance range of C_{sv} shown in Fig. 5. In general, the distance $[f_{h,HB}-f_{h,LB}]$ is getting wider as Z_1 is increasing and vice versa, where $f_{h,LB}$ and $f_{h,HB}$ are the highest center frequencies of the tunable filter in the LB and HB states, respectively. To locate $f_{evh,LB}$ and $f_{evh,HB}$ at desired values, the electrical parameters of a short-circuited stub, Z_{S1} and θ_{S1}, are carefully selected and C_{od} needs to be adjusted in order to make the relations, $f_{h,LB}$=($f_{odh,LB}$+$f_{evh,LB}$)/2 and $f_{h,HB}$=($f_{odh,HB}$+$f_{evh,HB}$)/2. Thereafter, the separation between the two resonant frequencies in each different center frequency can be maintained constant by changing C_{sv} and C_{od} as shown in Fig. 7. As a result, the separation between the two resonant frequencies is controllable, and the proposed resonator is suitable for the design of the widely tunable filter with a constant ABW. The overall tuning range of the resonator both in low- and high-band state is limited by the tuning range of C_L, which is varied from 5 pF to a maximum of 30 pF (6:1). However, the proposed resonator using switched varactors extends the tunable range by a factor or almost two times.

C. EXTERNAL COUPLING AND DESIGN PROCEDURE

To tune the center frequency f_c of the proposed 2-pole filter while maintaining a constant ABW over the entire

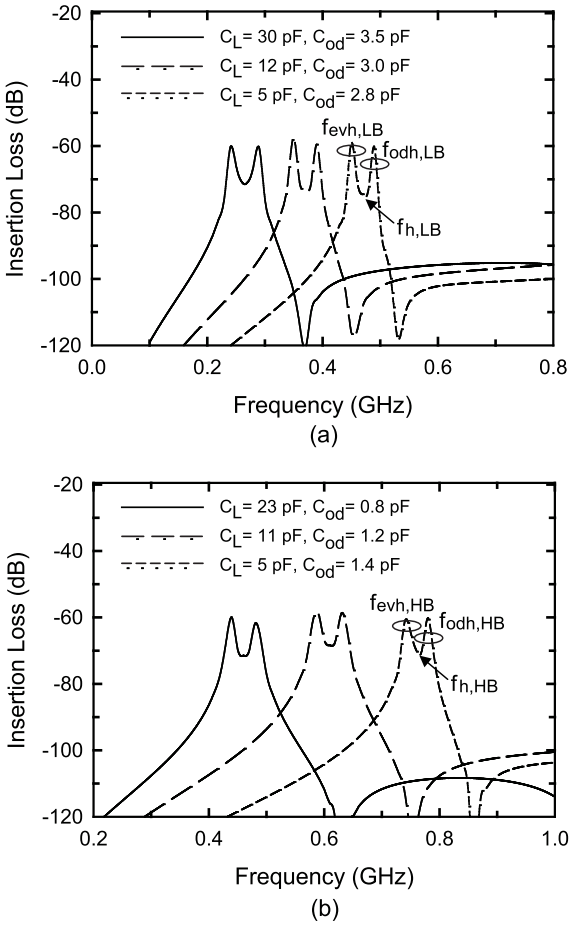

FIGURE 7. Resonant frequencies of the proposed switchable resonator according to C_L and C_{od} at (a) low-band and (b) high-band states.

tuning range, the desired external quality factor Q_{ext} of the tunable filter becomes smaller as f_c decreases. The equivalent circuits for the odd and even modes are presented in Fig. 8(a) and (b) with I/O external coupling. The external quality factors for the odd-mode ($Q_{ext,od}$) and even-mode circuits ($Q_{ext,ev}$) can be extracted from the input reflection coefficients [14] as

$$Q_{ext,od} = \pi f_{od} \tau_{S11,od} \tag{3a}$$

$$Q_{ext,ev} = \pi f_{ev} \tau_{S11,ev} \tag{3b}$$

where $\tau_{S11,od}$ and $\tau_{S11,ev}$ are group delays of S_{11} at the f_{od} and f_{ev}, respectively. Based on the required fractional bandwidth (FBW) and (3), Q_{ext} and the coupling coefficients (k) can be determined by the element values of a low-pass filter prototype, where the basic element values are g_i, i=0, 1, 2, and 3, as follows:

$$Q_{ext} = \frac{g_o g_1}{FBW} = \frac{Q_{ext,od} + Q_{ext,ev}}{2}. \tag{4}$$

$$k = \frac{FBW}{g_1 g_2} = \frac{|f_{even} - f_{odd}|}{f_c}. \tag{5}$$

For design convenience, Q_{ext} of the filter is defined as the arithmetic average of $Q_{ext,od}$ and $Q_{ext,ev}$. A second-order

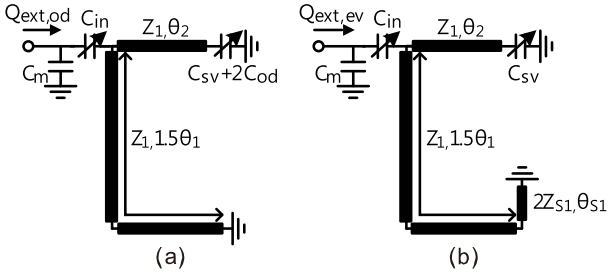

FIGURE 8. Equivalent circuits model of (a) odd-mode and (b) even-mode with I/O external couplings.

Chebyshev low-pass prototype with a 0.1-dB ripple level is chosen to acquire the proper Q_{ext} and k in order to design a tunable BPF with a 3-dB ABW of 75 MHz. To obtain the desired Q_{ext} over the tuning range, a variable capacitor, C_{in}, and a fixed capacitance, C_m, were utilized as shown in Fig. 8. The detailed frequency-dependent coupling-element values for the tunable filter are discussed in the next section.

As described above, the proposed resonator can control both even- and odd-mode resonant frequencies, and has the added capability of varying the odd-mode resonant frequency. Prior to the practical design of the tunable filter, the design procedures are introduced as follows.

1) The first step is to determine the requirement of the ideal switchable tunable dual-mode filter: The requirement for the separation between even- and odd-mode resonant frequencies should be established based on the selected low-pass filter prototype and FBW at each f_c.
2) The second step is to realize the frequency-tuning range of the low-band state and high-band state: The tuning ratio of the switchable resonator can be set by the electrical parameters of Z_{s2} and θ_{s2}, and a capacitance tuning range of C_L with a moderate Q.
3) The third step is to calculate the desired external quality factor Q_{ext} and coupling coefficient k: Based on the required FBW and low-pass filter prototype, the desired Q_{ext} and k can be specified from (4) and (5). The input-matching capacitors C_{in} and C_m are added to satisfy the requirement of Q_{ext} over the tuning range.
4) The fourth step is to optimize the final physical parameters of the proposed filter: The optimization was carried out using the full-wave EM simulation tools. Initially, the physical dimensions of the structure were derived from the line calculator in Advanced Design System (ADS). Then, we performed the EM simulation Iteratively, including all of the unexpected parasitic effects, via-hole, and coupling effects.

III. FILTER DESIGN AND EXPERIMENTAL VERIFICATION

A. FILTER IMPLEMENTATION

To validate the proposed structure, a 2-pole tunable filter was designed using the proposed switched varactor tuned resonator. To meet the desired Q_{ext}, the tapped-line input and output coupling were used with the separation between two

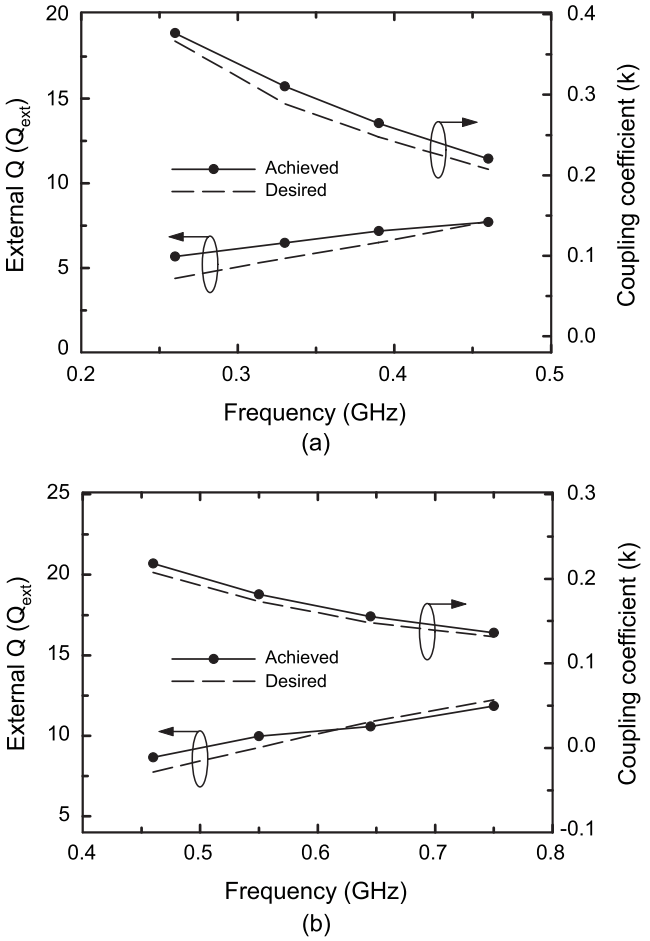

FIGURE 9. Desired and achieved Q_{ext} and k of (a) low-band state and (b) high-band state for a constant ABW.

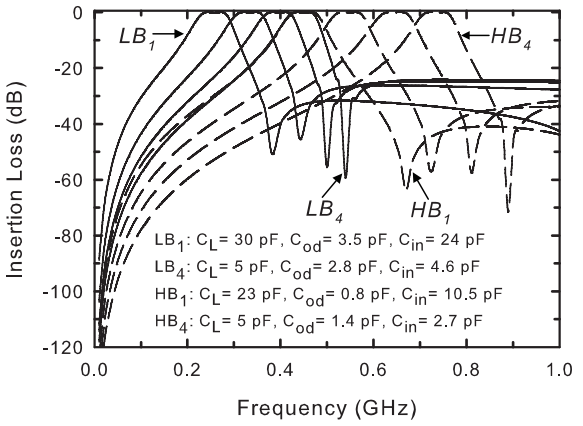

FIGURE 10. Circuit simulated S-parameters of the proposed tunable BPF: (a) low-band state, (b) high-band state.

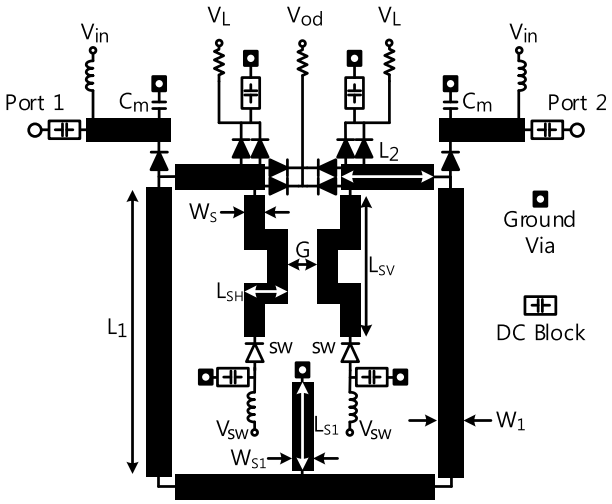

FIGURE 11. Layout of the designed tunable BPF.

resonant frequencies kept constant at 70 MHz at each tuned f_c. The tapped-line coupling is composed of a variable C_{in} that ranges from 4.6 pF to 24 pF in the low-band (LB) state when the switches are off, and from 2.7 pF to 10.5 pF in the high-band (HB) state when the switches are on, as well as a fixed C_m of 2 pF. From the specified low-pass prototype and the designed C_{in} and C_m, the desired and achieved k and Q_{ext} are depicted in Fig. 9, where the separation between two resonant frequencies is kept constant at 70 MHz at each tuned f_c. Fig. 10 shows the responses of the LB and HB state for different values of variable capacitances (C_L, C_{od}, and C_{in}) with a fixed C_m of 2 pF, where LB_1 and LB_4 are respectively the first and fourth bands of the LB state, whereas HB_1 and HB_4 are respectively the first and fourth bands of the HB state. Each transmission zero at higher side of the passbands is created by a two-path coupling between the upper path with C_{od} and the lower path with short-circuited stub (Z_{S1} and θ_{S1}).

Based on the above investigation, a tunable BPF is implemented and fabricated on a Rogers RO4003C substrate with a thickness of h=0.81 mm, a dielectric constant of ϵ_r=3.38, and a loss tangent of $\tan\delta$=0.0027. Varactor and p-i-n diodes from Skyworks were used to implement the variable capacitors and switches in Fig. 11, where SMV 1130 for C_L, SMV 1233 for C_{od}, SMV 1801 for C_{in}, and SMP 1322 for switches. An inductor of 220 nH and resistors of 20 kΩ are chosen to bias the p-i-n diode switches and varactor diodes, respectively. C_m is a matching capacitor with a capacitance of 2 pF, and DC block capacitors are 200 pF with a self-resonance frequency higher than 800 MHz. We used varactors, C_L and C_{od} in parallel in order to obtain the desired capacitance ranges. The dimensions of the filter were determined as in Table 2. The hole-vias were also used to provide a ground connection. A photograph of the proposed tunable BPF is shown in Fig. 12, where the filter has a very compact size of 49.5 mm × 36.5 mm (i.e., $0.2\lambda_g \times 0.14\lambda_g$, where λ_g is the guided wavelength of the microstrip structure at 725 MHz, which is the highest center frequency).

B. MEASURED RESULTS

Fig. 13 shows the measured results of the filter, where the s-parameters are measured using an Agilent E8364A network analyzer. The internal bias tees in the network analyzer are

TABLE 2. Physical dimensions of the designed tunable filter.

W_1	L_1	L_2	W_{s1}	L_{s1}	W_{s2}	L_{s2v}	L_{s2H}	G
3.2	19	7.2	1.2	5.8	0.6	8.2	2.2	0.8

All units are in millimeters.

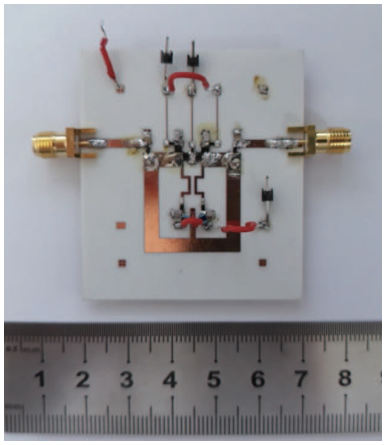

FIGURE 12. Photograph of the designed BPF.

used for V_{in} to bias the input/output coupling varactor. When the two switches are turned off, the proposed filter operating in the low-band state shows a frequency-tuning range from 255 MHz to 455 MHz by controlling bias voltages of V_L, V_{od}, and V_{in}, as shown in Fig. 13, where the detail bias voltages are also written. The measured (simulated) insertion loss and 3-dB bandwidth are 1.4−1.8 dB (0.8−1.3 dB) and 73±3 MHz (76±2 MHz), respectively, with a return loss lower than −10 dB. When the switches are turned on, the results of the proposed filter in the high-band state show a frequency-tuning range from 455 MHz to 725 MHz by adjusting bias voltages of V_L, V_{od}, and V_{in} as depicted in Fig. 13. The measured (simulated) insertion loss and 3-dB bandwidth are 2.5−2.9 dB (0.9−1.9 dB) and 76±6 MHz (78±4 MHz), respectively, with a return loss lower than −12 dB. As a result, the proposed tunable BPF has a wide frequency-tuning ratio of 2.85 with a constant ABW. The insertion losses and the ABW values are summarized in Fig. 14 for both low- and high-band states.

The third-order intercept point (IIP_3) and input 1-dB gain compression point (P_{1dB}) are also measured at different values of f_c over the tuning range using the Agilent Technology ESG Vector signal generator and Anritsu ProtekA734A spectrum analyzer. The measured results of IIP_3 with a 1-MHz offset and the input P_{1dB} for different f_c are shown in Fig 15. The IIP_3 and input P_{1dB} range from 5.2 dBm to 25.8 dBm and from 1.5 dBm to 21.1 dBm, respectively, as the f_c varies from 255 MHz to 725 MHz. These values are limited by nonlinearities of the p-i-n diode switches and varactor diodes. The p-i-n diode switches that are turned off in the low-band state are the main limiting factors owing to the high voltage swing at the open stub. To increase the power-handling capability, the p-i-n diode switches need to be stacked or replaced with RF MEMS switches.

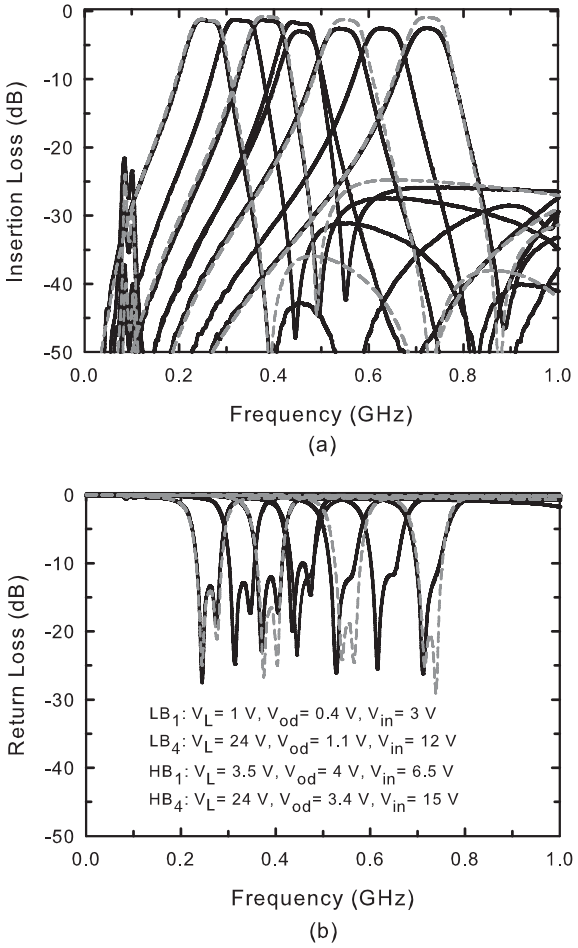

FIGURE 13. Measured and simulated S-parameters of the fabricated filter. (a) insertion loss, (b) return loss (solid line: Measurement, dashed line: Simulations).

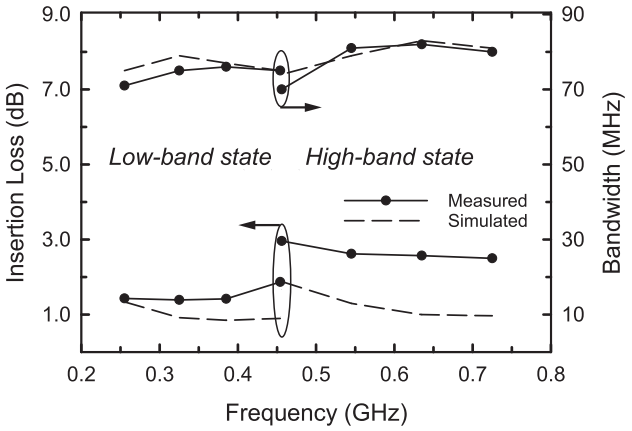

FIGURE 14. Measured and simulated insertion loss and ABW versus different f_c in both states.

IV. EXTENSION TO 4-POLE FILTER DESIGN

The proposed 2-pole tunable filter can be applied to a 4-pole tunable configuration based on the topology in Fig. 16.

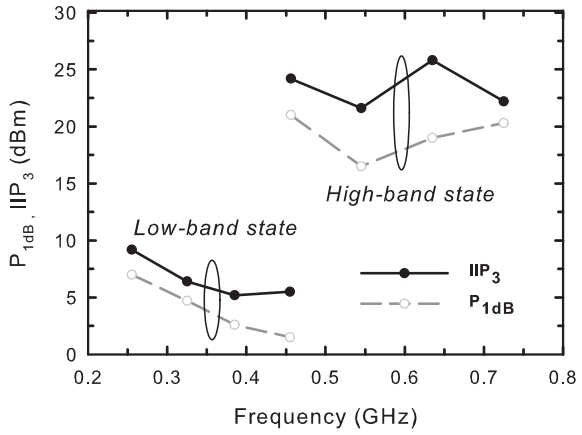

FIGURE 15. Measured P1dB and IIP3 versus different f_c in both states.

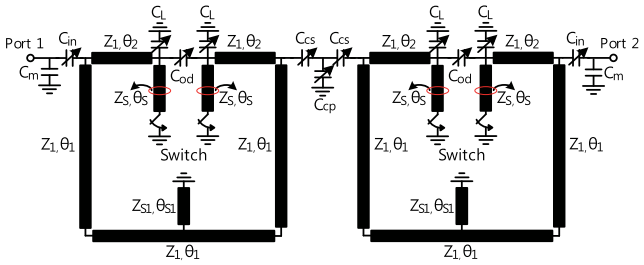

FIGURE 16. Configuration of the proposed tunable 4-pole BPF.

Because the measured results of the fabricated 2-pole filter agree well with the simulated ones, we can estimate the measured results of 4-pole filter by extracting the simulated ones. The coupling between the two 2-pole filters is done using tunable T network which is composed of C_{cs} and C_{cp}. The simulated responses of the 4-pole and 2-pole tunable BPFs are shown in Fig. 17 with almost the same center frequencies and bandwidths as those of the 2-pole filter, and the stopband performance is much better than that of the 2-pole filter as expected. The tuning range for the 4-pole filter operating in the low-band state shows a range from 250 MHz to 445 MHz. The simulated insertion loss and 3-dB bandwidth are 1.6−2.5 dB and 70±5 MHz, respectively, with a return loss lower than −11 dB. The operating frequencies of the 4-pole filter in the high-band state range from 440 MHz to 730 MHz. The simulated insertion loss and 3-dB bandwidth are 1.9−4.1 dB and 75±5 MHz, respectively, with a return loss lower than −12 dB. As a result, the 4-pole tunable BPF can also have a wide frequency-tuning ratio of 2.92 with a constant ABW.

Table 3 shows a comparison of the proposed tunable BPFs to other previously reported tunable BPFs. BPF I and II are the fabricated 2-pole tunable filter and the simulated 4-pole tunable filter, respectively. Among the BPFs in the table, the proposed BPF I and II have the widest frequency tuning ratio. In addition, they feature the compact sizes, low insertion losses and use moderate number of varactors compared to other BPFs.

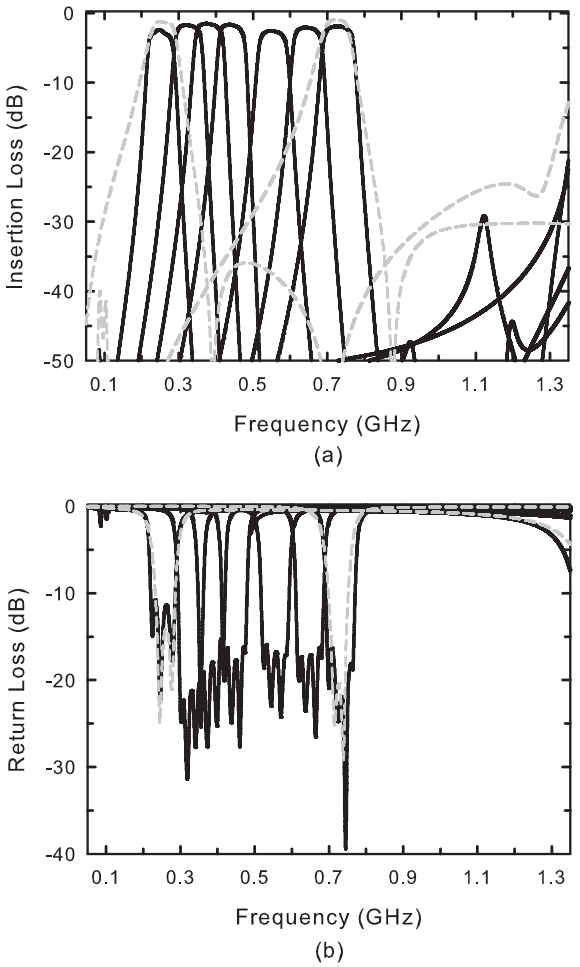

FIGURE 17. Simulated S-parameters of the tunable filters. (a) insertion loss, (b) return loss (solid line: 4-pole filter, dashed line: 2-pole filter).

TABLE 3. Comparison between the proposed and other previously reported tunable BPFs.

	Filter order	Insertion loss (dB)	Tuning ratio	Num. of varactors	Size† (λ_g^2)
BPF I	2	1.4−2.9	2.85	5	0.028
BPF II*	4	1.6−4.1	2.92	11	0.056
[3]	2	1.9−2.9	1.46	2	0.013
[8]	2	4.4−6.1	1.91	7	0.083
[21]	2	2.4−2.8	1.63	3	0.065
[22]	2	1.1−2.8	1.69	4	0.103
[9]	3	3.1−6.5	1.47	7	0.064
[4]	4	3.5−4.4	1.56	4	0.271
[19]	4	4.4−6.6	2.06	19	0.456

*Simulated results. †Estimated values at the highest center frequency of each tunable BPF using linecal.

V. CONCLUSION

This paper introduces a compact tunable BPF with a wide tuning ratio greater than one octave. Using the proposed switched varactors, we can overcome the limited tunability

of varactor diodes. To keep the ABW constant, the tapped-line input and output coupling were applied to obtain a good impedance match. The measured results were in good agreement with simulation results. As an extension, the proposed tunable BPF is applied for a 4-pole tunable one. They show that the proposed filters are attractive options for modern and future wireless communication systems.

REFERENCES

[1] C. Schuster, A. Wiens, F. Schmidt, M. Nickel, M. Schüßler, R. Jakoby, and H. Maune, "Performance analysis of reconfigurable bandpass filters with continuously tunable center frequency and bandwidth," *IEEE Trans. Microw. Theory Techn.*, vol. 65, no. 11, pp. 4572–4583, Nov. 2017.

[2] P. Sepidband and K. Entesari, "A CMOS wideband receiver resilient to out-of-band blockers using blocker detection and rejection," *IEEE Trans. Microw. Theory Techn.*, vol. 66, no. 5, pp. 2340–2355, May 2018.

[3] S. J. Park and G. M. Rebeiz, "Low-loss two-pole tunable filters with three different predefined bandwidth characteristics," *IEEE Trans. Microw. Theory Techn.*, vol. 56, no. 5, pp. 1137–1148, May 2008.

[4] D. Tian, Q. Feng, and Q. Xiang, "Synthesis applied 4^{th}-order constant absolute bandwidth frequency-agile bandpass filter with cross-coupling," *IEEE Access*, vol. 6, pp. 72287–72294, Nov. 2018.

[5] F. Lin and M. Rais-Zadeh, "Continuously tunable 0.55–1.9-GHz bandpass filter with a constant bandwidth using switchable varactor-tuned resonators," *IEEE Trans. Microw. Theory Techn.*, vol. 65, no. 3, pp. 792–803, Mar. 2017.

[6] M. A. El-Tanani and G. M. Rebeiz, "Corrugated microstrip coupled lines for constant absolute bandwidth tunable filters," *IEEE Trans. Microw. Theory Techn.*, vol. 58, no. 4, pp. 956–963, Apr. 2010.

[7] G. Zhang, Y. Xu, and X. Wang, "Compact tunable bandpass filter with wide tuning range of centre frequency and bandwidth using short coupled lines," *IEEE Access*, vol. 6, pp. 2962–2969, Dec. 2017.

[8] C.-F. Chen, G.-Y. Wang, and J.-J. Li, "Microstrip switchable and fully tunable bandpass filter with continuous frequency tuning range," *IEEE Microw. Wireless Compon. Lett.*, vol. 28, no. 6, pp. 500–502, Jun. 2018.

[9] Y. Chiou and G. M. Rebeiz, "A tunable three-pole 1.5-2.2-GHz bandpass filter with bandwidth and transmission zero control," *IEEE Trans. Microw. Theory Techn.*, vol. 59, no. 11, pp. 2872–2878, Nov. 2011.

[10] X.-G. Wang, Y.-H. Cho, and S.-W. Yun, "A tunable combline bandpass filter loaded with series resonator," *IEEE Trans. Microw. Theory Techn.*, vol. 60, no. 6, pp. 1569–1576, Jun. 2012.

[11] H.-J. Tsai, N.-W. Chen, and S.-K. Jeng, "Center frequency and bandwidth controllable microstrip bandpass filter design using loop-shaped dual-mode resonator," *IEEE Trans. Microw. Theory Techn.*, vol. 61, no. 10, pp. 3590–3600, Oct. 2013.

[12] X. Luo, S. Sun, and R. B. Staszewski, "Tunable bandpass filter with two adjustable transmission poles and compensable coupling," *IEEE Trans. Microw. Theory Techn.*, vol. 62, no. 9, pp. 2003–2013, Sep. 2014.

[13] T. Yang and G. M. Rebeiz, "Tunable 1.25–2.1-GHz 4-pole bandpass filter with intrinsic transmission zero tuning," *IEEE Trans. Microw. Theory Techn.*, vol. 63, no. 5, pp. 1569–1578, Sep. 2015.

[14] F.-C. Chen, R.-S. Li, and J.-P. Chen, "A tunable dual-band bandpass-to-bandstop filter using p-i-n diodes and varactors," *IEEE Access*, vol. 6, pp. 46058–46065, 2018.

[15] C.-C. Cheng and G. M. Rebeiz, "High-Q 4-6-GHz suspended stripline RF MEMS tunable filter with bandwidth control," *IEEE Trans. Microw. Theory Techn.*, vol. 59, no. 10, pp. 2469–2476, Oct. 2011.

[16] Y. Shim, Z. Wu, and M. Rais-Zadeh, "A high-performance continuously tunable MEMS bandpass filter at 1 GHz," *IEEE Trans. Microw. Theory Techn.*, vol. 60, no. 8, pp. 2439–2447, Aug. 2012.

[17] J. S. Sun, N. Kaneda, Y. Baeyens, T. Itoh, and Y.-K. Chen, "Multilayer planar tunable filter with very wide tuning bandwidth," *IEEE Trans. Microw. Theory Techn.*, vol. 59, no. 11, pp. 2864–2871, Nov. 2011.

[18] A. C. Guyette, "Intrinsically switched varactor-tuned filters and filter banks," *IEEE Trans. Microw. Theory Techn.*, vol. 60, no. 4, pp. 1044–1056, Apr. 2012.

[19] Y.-H. Cho and G. M. Rebeiz, "Tunable 4-pole noncontiguous 0.7–2.1-GHz bandpass filters based on dual zero-value couplings," *IEEE Trans. Microw. Theory Techn.*, vol. 63, no. 5, pp. 1579–1586, May 2015.

[20] B.-W. Min and G. M. Rebeiz, "Ka-band low-loss and high-isolation switch design in 0.13-μm CMOS," *IEEE Trans. Microw. Theory Techn.*, vol. 56, no. 6, pp. 1364–1371, Jun. 2008.

[21] C.-W. Tang, C.-T. Tseng, and S.-C. Chang, "Design of the compact tunable filter with modified coupled lines," *IEEE Trans. Compon., Packag., Manuf. Technol.*, vol. 4, no. 11, pp. 1815–1821, Nov. 2014.

[22] W. Qin, J. Cai, Y.-L. Li, and J.-X. Chen, "Wideband tunable bandpass filter using optimized varactor-loaded SIRs," *IEEE Microw. Wireless Compon. Lett.*, vol. 27, no. 9, pp. 812–814, Sep. 2017.

MINJAE JUNG was born in Daegu, South Korea, in 1988. He received the B.S. degree in electrical and electronics engineering from Chung-Ang University, Seoul, South Korea, in 2013. He is currently pursuing the Ph.D. degree with Yonsei University, Seoul.

His research interests include wideband/tunable microwave filters for cognitive-radio communication systems and millimeter-wave ICs for phased-array antenna applications.

BYUNG-WOOK MIN (S'03–M'08) was born in Seoul, South Korea. He received the B.S. degree from Seoul National University, Seoul, in 2002, and the M.S. and Ph.D. degrees from the University of Michigan at Ann Arbor, USA, in 2004 and 2007, respectively.

From 2006 to 2007, he was a Visiting Scholar with the University of California at San Diego, La Jolla. He is currently an Associate Professor with the Department of Electrical and Electronic Engineering, Yonsei University, Seoul. From 2008 to 2010, he was a Senior Engineer with Qualcomm Inc., Santa Clara, CA, USA, and Austin, TX, USA. His research interests include Si/SiGe RFIC and communication systems for microwave and millimeter-wave applications.